Eulerian-Lagrangian discontinuous Galerkin method for transport problems and its application to nonlinear Vlasov and incompressible dynamics

Jing-Mei Qiu

Department of Mathematical Sciences
University of Delaware
Joint work with S. Boscarino, X. Cai, W. Guo, and Y. Yang

Holistic Design of Time-Dependent PDE Discretizations, ICERM, Jan. 2022.

Keywords: Semi-Lagrangian, Arbitrary Lagrangian-Eulerian, Method-of-lines, RK exponential integrators, kinetic and incompressible fluid models

Outline

Motivation: Vlasov-Poisson system

A collisionless plasma in 1D1V can be described by the nonlinear Vlasov-Poisson system:

$$f_t + \mathbf{v} \cdot \nabla_{\mathbf{x}} f + \mathbf{E} \cdot \nabla_{\mathbf{v}} f = 0,$$
$$\mathbf{E} = -\nabla_{\mathbf{x}} \phi, \quad -\Delta_{\mathbf{x}} \phi = \rho - 1.$$

- $f(t, \mathbf{x}, \mathbf{v})$: the probability of finding a particle with velocity $\mathbf{v}$ at position $\mathbf{x}$ at time t.
- $\mathbf{E}$: electric field.
- $\rho = \int f \, d\mathbf{v}$: the macroscopic charge density.

Motivation: incompressible Euler equation in vorticity stream function formulation

Incompressible Navier Stokes equation:

$$\boxed{\mathbf{u}_t + \nabla \cdot (\mathbf{u} \otimes \mathbf{u} + p\mathbf{I}) = \frac{1}{Re}\Delta \boldsymbol{u}, \quad \nabla \cdot \boldsymbol{u} = 0.}$$

Applying the $\nabla\times$ operator to the $\mathbf{u}$ equation, we obtain the incompressible Navior-Stokes equation in vorticity stream function formulation

$$\begin{aligned}
&\omega_t + \nabla \cdot (\mathbf{u}\omega) = \frac{1}{Re}\Delta\omega \\
&\Delta\Phi = \omega,\ \ \mathbf{u} = \nabla^{\perp}\Phi = (-\Phi_y, \Phi_x).
\end{aligned}$$

Existing numerical methods

- Lagrangian approach:
  - Tracking macro-particle trajectories, e.g., Particle-in-cell (PIC).
  - For high-D problems with good qualitative results at low cost.
  - Inherent numerical noise $O(1/\sqrt{N})$: difficult to get precise results in some situations.
- Eulerian approach:
  - Grid-based scheme.
  - arbitrary order of accuracy in both space and time.
  - CFL restriction for stability with explicit time-stepping method.
- Semi-Lagrangian (SL) approach:
  - Combination of Eulerian approach and Lagrangian approach.
  - Grid-based scheme.
  - Numerical solution is updated by following trajectories.
  - Allowing very large CFL number.

- Eulerian approach:
  - Grid-based scheme.
  - Arbitrary order of accuracy in both space and time.

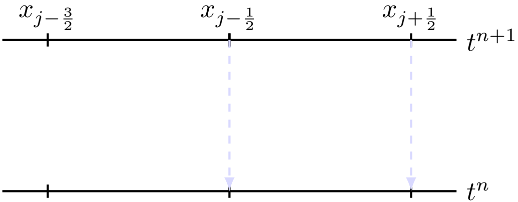

  - Consider $u_t + f(u)_x = 0$ solved by RKDG*.
  - $\int_{I_j} u_t \psi dx - \int_{I_j} f(u)\psi_x dx + (\hat{f}\psi^-)_{j+\frac{1}{2}} - (\hat{f}\psi^+)_{j-\frac{1}{2}} = 0.$
  - A limitation: The RKDG scheme suffers the stringent CFL stability restriction $\approx \frac{1}{2k+1}$.

*Cockburn and Shu, 80's

- Eulerian approach:
  - Grid-based scheme.
  - Arbitrary order of accuracy in both space and time.

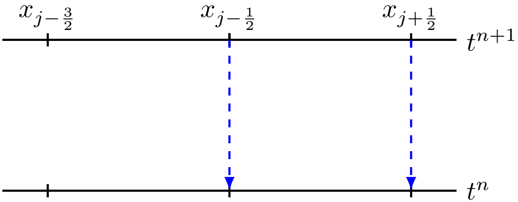

  - Consider $u_t + f(u)_x = 0$ solved by RKDG*.
  - $\int_{I_j} u_t \psi dx - \int_{I_j} f(u)\psi_x dx + (\hat{f}\psi^-)_{j+\frac{1}{2}} - (\hat{f}\psi^+)_{j-\frac{1}{2}} = 0.$
  - A limitation: The RKDG scheme suffers the stringent CFL stability restriction $\approx \frac{1}{2k+1}$.

*Cockburn and Shu, 80's

- Semi-Lagrangian (SL) approach:
  - Combination of Eulerian approach and Lagrangian approach.
  - Grid-based scheme.
  - Numerical solution is updated by following trajectories.
  - Allow very large CFL number.
  - Popular in plasma physics and global multi-tracer transport in atmospheric modeling.

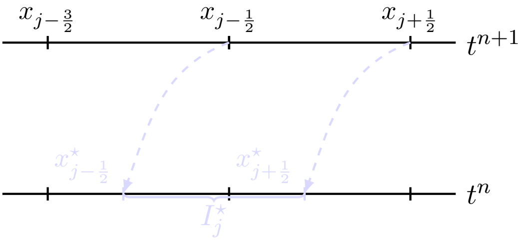

Figure: Backward SL.

- Semi-Lagrangian (SL) approach:
  - Combination of Eulerian approach and Lagrangian approach.
  - Grid-based scheme.
  - Numerical solution is updated by following trajectories.
  - Allow very large CFL number.
  - Popular in plasma physics and global multi-tracer transport in atmospheric modeling.

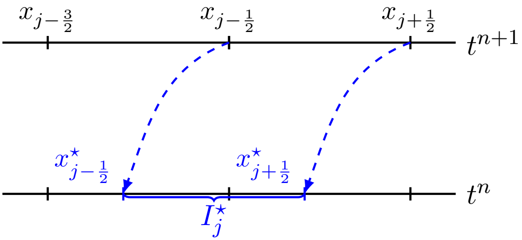

Figure: Backward SL.

SL schemes

SLDG method:

- DG: Low numerical dissipation; compactness; flexibility for boundary and parallel implementation; superconvergence.
- SL: Could take extra large time stepping size with accuracy and stability, leading to gain in efficiency.

Applications

- Plasma application: Vlasov equation.
- Climate modeling
- Fluid and kinetic models.

1D SLDG for the linear transport equation[†]

Consider a 1D linear transport problem

$$\frac{\partial u}{\partial t} + \frac{\partial}{\partial x}(a(x,t)u) = 0$$

with appropriate initial and boundary conditions.

We consider **an adjoint problem for the test function $\psi(x,t)$**:

$$\begin{cases} \psi_t + a(x,t)\psi_x = 0, \\ \psi(t = t^{n+1}) = \Psi(x), \end{cases}$$

which is in an advective form, hence ψ stays constant along the characteristics.

[†]Cai-Guo-Q., JSC, 2017

It can be shown that

$$\frac{d}{dt}\int_{\widetilde{I}_j(t)} u(x,t)\psi(x,t)dx = 0, \tag{1}$$

where $\widetilde{I}_j(t)$ is a dynamic interval bounded by characteristics emanating from cell boundaries of I_j at $t = t^{n+1}$.

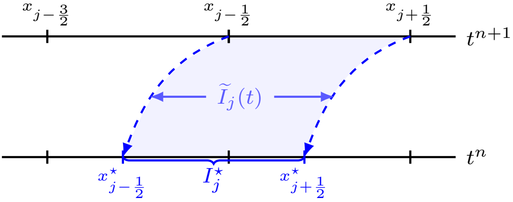

Thus, from equation (1),

$$\boxed{\int_{I_j} u(x,t^{n+1})\Psi(x,t^{n+1})dx = \int_{I_j^\star} u(x,t^n)\psi(x,t^n)dx.}$$

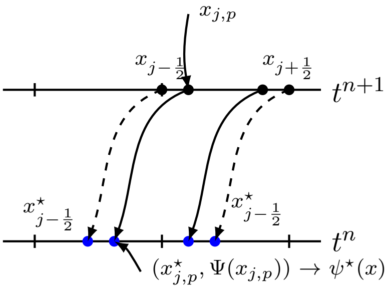

Two dimensional SLDG[§]

- Consider a two-dimensional linear transport problem

$$\frac{\partial u}{\partial t} + \frac{\partial}{\partial x}(a(x,y,t)u) + \frac{\partial}{\partial y}(b(x,y,t)u) = 0$$

  with appropriate initial and boundary conditions.

- Weak formulation of characteristic Galerkin method[‡]: an adjoint problem for the test function $\psi(x,y,t)$

$$\begin{cases} \psi_t + a(x,y,t)\psi_x + b(x,y,t)\psi_y = 0, \\ \psi(t = t^{n+1}) = \Psi(x,y). \end{cases}$$

  Then it can be shown that $\forall \psi \in P^k(A_j)$,

$$\frac{d}{dt}\int_{\widetilde{A}_j(t)} u(x,y,t)\psi(x,y,t)dxdy = 0$$

  with $\widetilde{A}_j(t)$ a dynamic interval bounded by characteristics emanating from cell boundaries of A_j at $t = t^{n+1}$.

[‡] Guo, Nair and Q., MWR, 2014.

[§] Cai, Guo and Q., JSC, 2017.

$$\boxed{\int_{A_j} u(x,y,t^{n+1})\Psi(x,y)dxdy = \int_{A_j^*} u(x,y,t^n)\psi(x,y,t^n)dxdy}$$

with A_j and $A_j^\star$ are shown as in the below left plot.

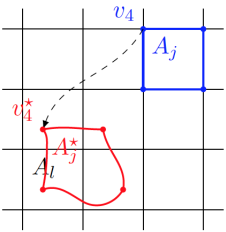

- Characteristics tracing: Locate four vertices of upstream cell $A_j^\star$: $v_q^\star(q=1,2,3,4)$ by solving the characteristics equations,

$$\begin{cases} \frac{dx(t)}{dt} = a(x(t),y(t),t), \\ \frac{dy(t)}{dt} = b(x(t),y(t),t), \\ x(t^{n+1}) = x(v_q), \\ y(t^{n+1}) = y(v_q), \end{cases}$$

starting from the four vertices of A_j: $v_q(q=1,2,3,4)$.

Evaluation of $\int_{A_j^\star} u(x,y,t^n)\psi(x,y,t^n)dxdy$

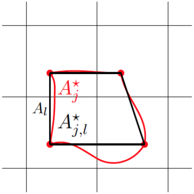

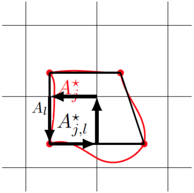

Two observations:

- $\psi(x,y,t^n)$ may not be a polynomial.
- $u(x,y,t^n)$ is a piecewise polynomial function on background cells.

Strategies:

- Reconstruct $\psi^\star(x,y)$ approximating $\psi(x,y,t^n)$ on $A_j^\star$ by a least square strategy, based on

$$\psi(x(v_q^\star),y(v_q^\star),t^n) = \Psi(x(v_q),y(v_q)),$$

  $q = 1,2,3,4.$

- Evaluation of the integrand over the upstream cell has to be done subregion-by-subregion.

The swirling deformation problem.

$$u_t - \left(\cos^2(\frac{x}{2})\sin(y)g(t)u\right)_x + \left(\sin(x)\cos^2(\frac{y}{2})g(t)u\right)_y = 0,$$

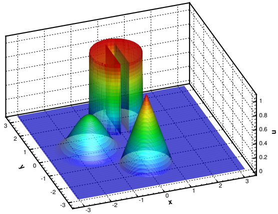

with

- $g(t) = \cos\left(\frac{\pi t}{T}\right)\pi,$
- $x \in [-\pi, \pi],\ y \in [-\pi, \pi],$
- The initial condition as shown on the right.

Shapes of upstream cells

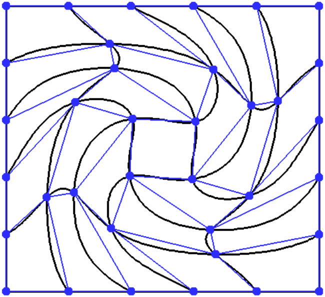

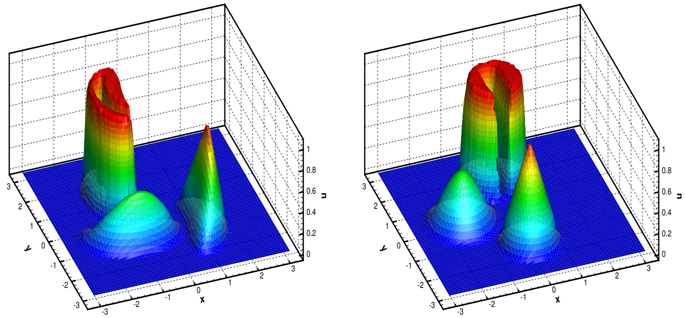

Figure: Swirling deformation problem. Third order SL DG scheme: $T = 0.75$ (left) and $T = 1.5$ (right). The numerical mesh is 80×80 with $CFL = 5$.

The swirling deformation problem: convergence study

Table: $u_t - \left(\cos^2\left(\frac{x}{2}\right)\sin(y)\cos\left(\frac{2\pi t}{3}\right)\pi u\right)_x + \left(\sin(x)\cos^2\left(\frac{y}{2}\right)\cos\left(\frac{2\pi t}{3}\right)\pi u\right)_y = 0.$
The initial condition is a smooth cosine bell. $T = 1.5$.

Mesh	L^2 error	Order	L^2 error	Order
P^1 SLDG	CFL $=\pi$		CFL $=5\pi$	
20×20	1.25E-02		8.59E-03	
40×40	2.92E-03	2.10	2.14E-03	2.00
80×80	5.96E-04	2.29	5.42E-04	1.98
160×160	1.30E-04	2.20	1.33E-04	2.02
P^2 SLDG				
20×20	3.22E-03		9.37E-03	
40×40	6.58E-04	2.29	2.87E-03	1.71
80×80	1.42E-04	2.22	6.92E-04	2.05
160×160	3.15E-05	2.17	1.89E-04	1.87
P^2 SLDG-QC				
20×20	2.61E-03		5.29E-03	
40×40	3.15E-04	3.05	7.78E-04	2.77
80×80	3.81E-05	3.05	1.04E-04	2.90
160×160	4.91E-06	2.96	1.47E-05	2.83

Properties of the scheme

Convection equations in a conservative form

$$\boxed{u_t + \nabla_{\mathbf{x}} \cdot (\mathbf{a}u) = 0.}$$

A SLDG discretization of

$$\boxed{u^{n+1} = SLDG(\mathbf{a}, \Delta t)u^n.}$$

- Mass conservation.
- High order accuracy in space and time.
- Unconditionally stability which allows arbitrary large stepping size.
- No dimensional splitting error for multi-dimensional problems.

Motivation of ELDG

- Motivation
  - Higher dimensional problem: complication from quadratic curve approximations to sides of upstream cells.
  - General nonlinear problems: characteristics tracing is difficult or impossible.
- Related work in literature
  - Eulerian-Lagrangian localized adjoint methods (ELLAM): Douglas and Russel (82'), Celia, Ewing, Wang, etc.
  - Eulerian-Lagrangian WENO method: Huang, Arbogast, et. al. 2016
  - Arbitrary Lagrangian-Eulerian (ALE) moving mesh method.

The space-time region of ELDG

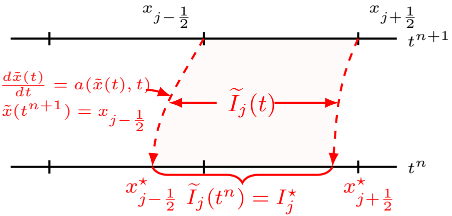

$$\frac{d}{dt}\int_{\widetilde{I}_j(t)} u(x,t)\psi(x,t)dx = 0.$$

- Linear function $\alpha(x,t)$ in approximating $a(x,t)$.
- Feature I: Ω_j: trapezoid; in high-D upstream cells are polygons (tetrahedron).
- Feature II: straight lines approximating characteristics.

The space-time region of ELDG

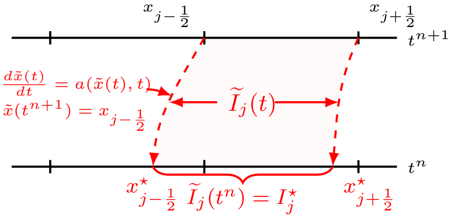

$$\frac{d}{dt}\int_{\widetilde{I}_j(t)} u(x,t)\psi(x,t)dx = 0.$$

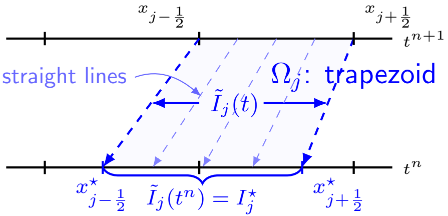

- Linear function $\alpha(x,t)$ in approximating $a(x,t)$.
- Feature I: Ω_j: trapezoid; in high-D upstream cells are polygons (tetrahedron).
- Feature II: straight lines approximating characteristics.

ELDG for 1D linear transport: A modified adjoint problem

- We consider

$$u_t + (a(x,t)u)_x = 0. \tag{2}$$

- We consider the adjoint problem with $\forall \Psi \in P^k(I_j)$ on the time interval $[t^n, t^{n+1}]$:

$$\begin{cases} \psi_t + \alpha(x,t)\psi_x = 0, \ t \in [t^n, t^{n+1}], \\ \psi(t = t^{n+1}) = \Psi(x), \end{cases} \tag{3}$$

with $\alpha(x,t)$ being a linear approximation to the original velocity field $a(x,t)$.

The semi-discrete ELDG scheme

$$\int_{\Omega_j} [(2)\cdot\psi + (3)\cdot u]\, dxdt = 0.$$

Transform the time integral form to the time differential form gives

$$\boxed{\frac{d}{dt}\int_{\tilde{I}_j(t)} (u\psi)dx = -\left(F\psi\right)\Big|_{\tilde{x}_{j+\frac{1}{2}}(t)} + \left(F\psi\right)\Big|_{\tilde{x}_{j-\frac{1}{2}}(t)} + \int_{\tilde{I}_j(t)} F\psi_x dx.} \quad (4)$$

where $F(u) \doteq (a-\alpha)u$.

- In special case of $\alpha(x,t)=0$, ELDG becomes RKDG;
- In special case of $\alpha(x,t)=a(x,t)$, ELDG becomes SLDG.
- The time differential form allows for the direct application of method-of-lines SSP RK methods.

The semi-discrete ELDG scheme (cont.)

$$\boxed{\frac{d}{dt}\int_{I_j}(u\Psi(\xi))\frac{\partial\tilde{x}(t;(\xi,t^{n+1}))}{\partial\xi}d\xi = -\left(\hat{F}\Psi\right)\Big|_{\xi=x_{j+\frac{1}{2}}} + \left(\hat{F}\Psi\right)\Big|_{\xi=x_{j-\frac{1}{2}}} + \int_{I_j}F\Psi_\xi d\xi.}$$

- Lax-Friedrich flux:
  $\hat{F}(u^-,u^+) = \frac{1}{2}(F(u^-)+F(u^+)) + \frac{\alpha_0}{2}(u^- - u^+), \alpha_0 = \max_u |F'(u)|.$
- $k+1$ points Gauss quadrature rules :
  $\int_{I_j}F(u_h)\Psi_\xi d\xi \approx \sum_{l=1}^{k+1}(F(u_h(x_{jl},t))\Psi_\xi(x_{jl})\omega_l\Delta x),$

Fully discrete ELDG: SSP RK time discretization

- Denote $\tilde{U}_h = \int_{\tilde{I}_j(t)} u\psi dx = \int_{I_j} u_h \Psi J d\xi$ with $J = \frac{\partial \tilde{x}(t;(\xi, t^{n+1}))}{\partial \xi}$;
- Denote the spatial discretization operator as $\mathcal{L}\left(\tilde{U}_h(t), t\right)$.

$$\frac{\partial}{\partial t}\tilde{U}_h(t) = \mathcal{L}\left(\tilde{U}_h(t), t\right), \text{with} \quad \tilde{U}_h(t^n) = \tilde{U}_h^n.$$

SSP RK methods:

1. Evaluate $\tilde{U}_h^n = \int_{I_j^\star} u(x, t^n)\psi(x, t^n)dx$ at t^n for all test functions Ψ by the SLDG scheme.
2. For RK stages $i = 1, \cdots, s$, compute

$$\tilde{U}_h^{(i)} = \sum_{l=0}^{i-1}\left[\alpha_{il}\tilde{U}_h^{(l)} + \beta_{il}\Delta t^n \mathcal{L}\left(\tilde{U}_h^{(l)}, t^n + d_l \Delta t^n\right)\right].$$

Order	α_{il}	β_{il}	d_l
3	1	1	0
	$\frac{3}{4}$ $\frac{1}{4}$	0 $\frac{1}{4}$	1
	$\frac{1}{3}$ 0 $\frac{2}{3}$	0 0 $\frac{2}{3}$	$\frac{1}{2}$

Allow for a large time step

- Similar to the time step of DG method, we may use the following time step

$$\Delta t \leq \frac{\Delta x}{(2k+1)\max|a(x,t)-\alpha(x,t)|}.$$

- $\alpha(x,t)$ in approximation of $a(x,t)$

$$\max|a(x,t)-\alpha(x,t)| = O(\Delta t) + O(\Delta x^2)$$

$$\Downarrow$$

$$\Delta t \sim \Delta x^{\frac{1}{2}},$$

to be verified by the numerical results.

A modified adjoint problem for 2D transport

- 2D linear transport equation:

$$u_t + (a(x,y,t)u)_x + (b(x,y,t)u)_y = 0.$$

- We consider a modified adjoint problem at $\tilde{A}_j(t)$ on the time interval $t \in [t^n, t^{n+1}]$:

$$\psi_t + \alpha(x,y,t)\psi_x + \beta(x,y,t)\psi_y = 0, \quad \psi(x,y,t=t^{n+1}) = \Psi(x,y) \in P^k(A_j),$$

  where (α, β) are Q^1 or P^1 polynomials on A_j at t^{n+1} approximating the original velocity field (a,b).

2D ELDG formulation

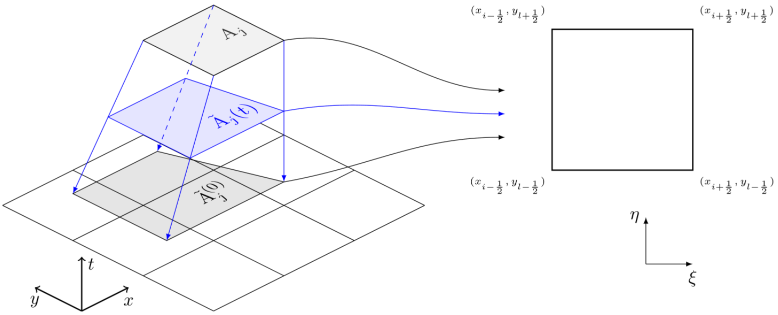

$$\frac{d}{dt}\int_{\tilde{A}_j(t)} u\psi dxdy = -\int_{\partial\tilde{A}_j(t)} \psi\hat{\mathbf{F}}\cdot\mathbf{n}dS + \int_{\tilde{A}_j(t)} \mathbf{F}\cdot\nabla\psi dxdy,$$

with

$$\mathbf{F}(u,x,y,t) = \begin{pmatrix} (a(x,y,t)-\alpha(x,y,t))u \\ (b(x,y,t)-\beta(x,y,t))u \end{pmatrix}.$$

2D ELDG formulation on the reference element

- Jacobian, $J(\xi,\eta) = \frac{\partial(\tilde{x},\tilde{y})}{\partial(\xi,\eta)}(\tau) = \begin{pmatrix} 1 - \frac{\partial\alpha}{\partial\xi}(t^{n+1}-\tau) & \frac{\partial\alpha}{\partial\eta}(t^{n+1}-\tau) \\ -\frac{\partial\beta}{\partial\xi}(t^{n+1}-\tau) & 1 - \frac{\partial\beta}{\partial\eta}(t^{n+1}-\tau) \end{pmatrix}$.
- Mapping formulas:
  - $dxdy = \det(J(\xi,\eta))d\xi d\eta$,
  - $\nabla_{x,y}\psi(x,y) = J(\xi,\eta)^{-1}\nabla_{\xi,\eta}\Psi(\xi,\eta)$,
  - $\mathbf{n}dS = \det(J(\xi,\eta))J(\xi,\eta)^{-T}\breve{\mathbf{n}}d\breve{S}$.

$$
\begin{aligned}
&\frac{d}{dt}\int_{A_j} u(\tilde{x}(t,(\xi,\eta,t^{n+1})),\tilde{y}(t,(\xi,\eta,t^{n+1})),t)\Psi(\xi,\eta)\det(J(\xi,\eta))d\xi d\eta \\
&= -\int_{\partial A_j} \Psi(\xi,\eta)\mathbf{F}\cdot\left(\det(J(\xi,\eta))J(\xi,\eta)^{-T}\breve{\mathbf{n}}\right)d\breve{S} \\
&+ \int_{A_j} \mathbf{F}\cdot(J(\xi,\eta)^{-1}\nabla_{\xi,\eta}\Psi)\det(J(\xi,\eta))d\xi d\eta.
\end{aligned}
$$

Similar to the procedure of 1D ELDG, SSP RK discretization can be applied to the above formulation.

EL RKDG on the unstructured mesh

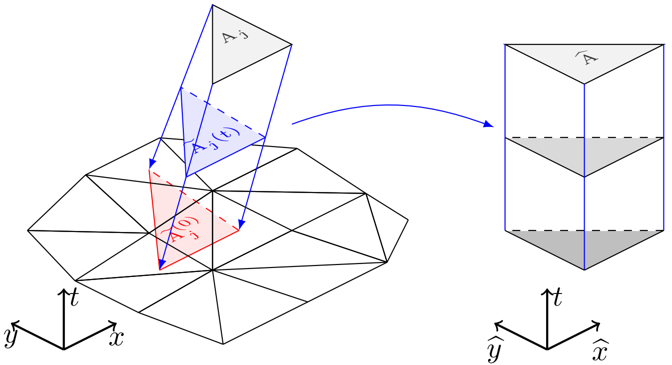

Summary: EL-RKDG

- An organic coupling of SL DG and Eulerian RK DG methods
  - Step 1 (SLDG): L^2 re-projection of solutions on upstream cells.
  - Step 2 (RKDG): flux differences between original and adjoint problems over the time-dependent dynamic volumes.
- A unified framework to accommodate both SL and RK DG methods.
  - RK DG: $\alpha = 0$.
  - SL DG: $\alpha(x, t)$ follows the exact characteristics.
- Let Δt_{ELDG} be stability constraint of the ELDG.

$$\Delta t_{ELDG} \in [\Delta t_{RKDG}, \Delta t_{SLDG}]$$

- High order accuracy, mass conservation, superconvergence, unstructured mesh.

1D transport equation with variable coefficients

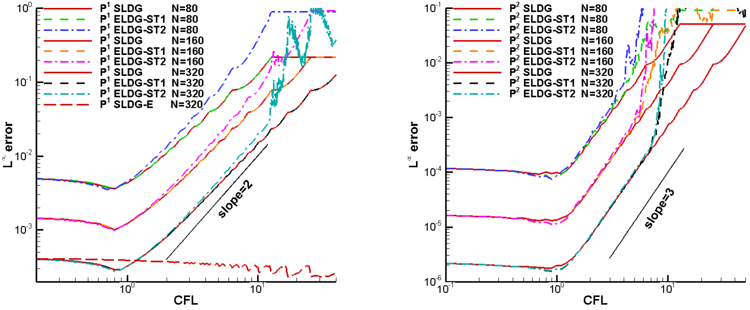

Figure: P^1 SLDG-E means P^1 SLDG scheme which solve the characteristic line exactly. Observations: (1) expected order of convergence in time is observed; (2) Stability bounds for the maximum CFLs of P^2 ELDG using $N = 80, 160, 320$ are observed to be around 3.5, 5 , 7 increasing at the ratio of $\sqrt{2} \approx 1.4$, which verifies the time step estimate $\Delta t \sim C\sqrt{\Delta x}$.

Rigid body rotation

$$u_t - (yu)_x + (xu)_y = 0$$

- A circle domain: $(x, y) \in \{(x, y) | x^2 + y^2 \leq \pi^2\}$
- A sample mesh with the mesh 160 (GMSH).

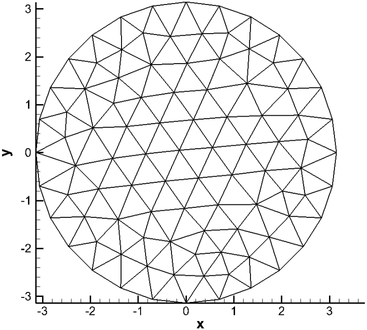

Rigid body rotation: high resolution

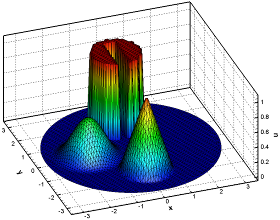

(a) initial state $N = 7432$

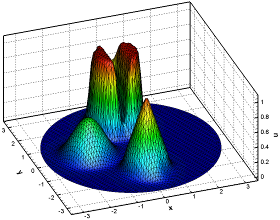

(b) P^2 RKDG, $CFL = 0.15$

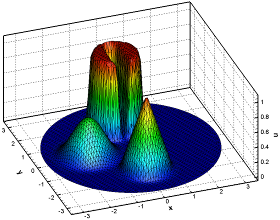

(c) P^2 SLDG, $CFL = 10.2$

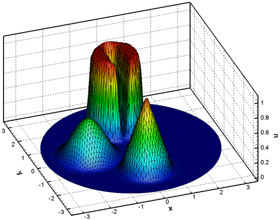

(d) P^2 ELDG, $CFL = 10.2$

Swirling deformation flow: high order spatial and temporal accuracy

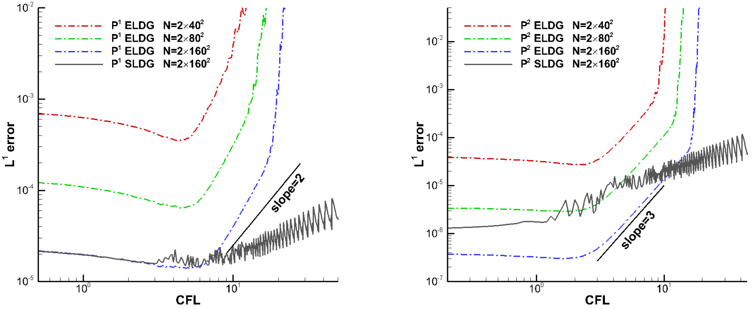

Figure: The swirling deformation flow with the smooth cosine bells with $T = 1.5$. High order spatial and temporal accuracy, large CFL range increase with mesh refinement.

Swirling deformation flow: DG P^2

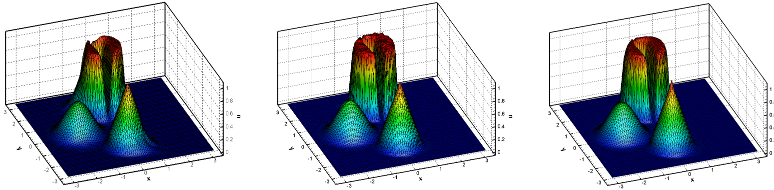

(a) RKDG, $CFL = 0.15$ (b) SLDG, $CFL = 10.2$ (c) ELDG, $CFL = 10.2$

SLDG-RKEI and ELDG-RKEI methods

- So far, SLDG and ELDG solvers are proposed for linear transport equations.
- In order to solve the following nonlinear transport problem

$$\boxed{u_t + \nabla_{\mathbf{x}} \cdot (\mathbf{P}(u; \mathbf{x}, t)u) = 0}$$

  we apply a high order Runge-Kutta exponential integrator[¶], which decomposes the equation into a set of linearized transport problems.
- The SL method can be viewed as an exact time integrator for linear transport problems.

[¶] Celledoni, et al., FGCS ,2003

RK exponential integrators for nonlinear ODE systems

Consider

$$\frac{dy(t)}{dt} = C(y)y, \quad y(t=0) = y_0. \tag{5}$$

A first order scheme

$$y^{n+1} = \exp(C(y^n)\Delta t)y^n. \tag{6}$$

To improve the accuracy, a class of commutator-free exponential integrators can be used. The idea is to achieve high order temporal accuracy via taking composition of a sequence of linear solvers by freezing coefficients, which can be explicitly computed as a linear combination of $C(Y)$ from previous RK stages.

$$\begin{aligned}
y^{(1)} &= y^n \\
y^{(2)} &= exp\left(\frac{1}{3}C(y^{(1)})\Delta t\right) y^{(1)} \\
y^{(3)} &= exp\left(\frac{2}{3}C(y^{(2)})\Delta t\right) y^{(1)} \\
y^{n+1} &= exp\left((-\frac{1}{12}C(y^{(1)}) + \frac{3}{4}C(y^{(3)}))\Delta t\right) y^{(2)}.
\end{aligned}$$

A third order SLDG-CF3C03 scheme

$$
\begin{aligned}
u^{(1)} &= u^n \\
u^{(2)} &= SLDG\left(\frac{1}{3}\mathbf{P}(u^{(1)}), \Delta t\right) u^{(1)} \\
u^{(3)} &= SLDG\left(\frac{2}{3}\mathbf{P}(u^{(2)}), \Delta t\right) u^{(1)} \\
u^{n+1} &= SLDG\left(-\frac{1}{12}\mathbf{P}(u^{(1)}) + \frac{3}{4}\mathbf{P}(u^{(3)}), \Delta t\right) u^{(2)}.
\end{aligned}
$$

The guiding center Vlasov model

The guiding center model describes a highly magnetized plasma in the transverse plane of a tokamak. It reads

$$\rho_t + \nabla \cdot (\mathbf{E}^{\perp}\rho) = 0,$$

$$-\Delta\Phi = \rho, \;\; \mathbf{E}^{\perp} = (-\Phi_y, \Phi_x)$$

where ρ is the charge density of the plasma and $\mathbf{E} = (E_1, E_2)$ determined by $\mathbf{E} = -\nabla\Phi$ is the electric field.

Guiding center Vlasov: high order spatial accuracy

Table: Guiding center Vlasov on the domain $[0, 2\pi] \times [0, 2\pi]$ with the initial condition $\omega(x, y, 0) = -2\sin(x)\sin(y)$. $T = 1$. $CFL = 1$. The temporal scheme CF3C03 is used.

Mesh	L^1 error	Order	L^1 error	Order
	P^1 SLDG		P^1 ELDG	
20^2	1.39E-02	–	9.59E-03	–
40^2	3.66E-03	1.93	2.35E-03	2.03
60^2	1.65E-03	1.97	1.02E-03	2.06
80^2	9.37E-04	1.96	5.78E-04	1.97
100^2	6.01E-04	1.99	3.69E-04	2.00
	P^2 SLDG-QC		P^2 ELDG	
20^2	2.13E-03	–	1.54E-03	–
40^2	2.73E-04	2.97	1.79E-04	3.10
60^2	8.11E-05	2.99	5.21E-05	3.05
80^2	3.48E-05	2.94	2.10E-05	3.16
100^2	1.77E-05	3.02	1.07E-05	3.04

Guiding center Vlasov: high order temporal accuracy & huge time step!

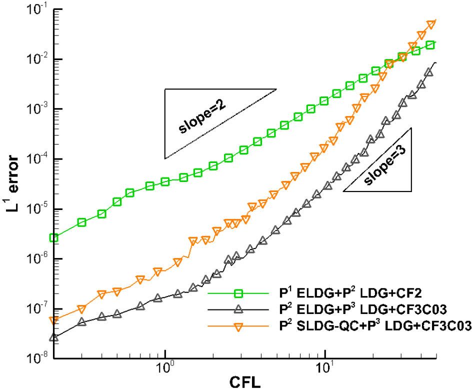

Figure: The Kelvin-Helmholtz instability problem at $T = 5$. The mesh of 120×120 cells is used. The reference solution from the corresponding scheme with $CFL = 0.1$.

SLDG-QC with adaptive time stepping algorithm for guiding center Vlasov

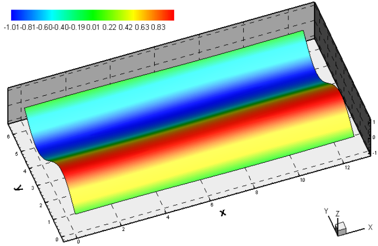

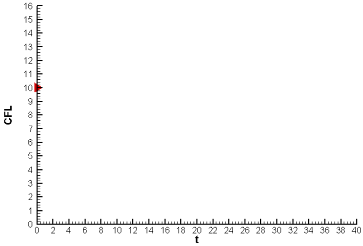

3D plot of solutions of third order SLDG-QC-RKEI method with the adaptive time-stepping algorithm based on the area invariant, $\max_j \left| \frac{\text{area}(A_j^\star) - \text{area}(A_j)}{\text{area}(A_j)} \right|$. The mesh is 100×100.

Summary

We propose an ELDG method, which avoids to construct a quadratic-curved quadrilaterals and still enjoys

- high order DG spatial discretization, high order temporal discretization, large time stepping size, mass conservation, resolution of filamentations, superconvergence of long time integration.
- SLDG + ALE + characteristics tracking/approximation

Current/future development and open problems

- Linear system such as the wave equation (joint work with Dr. X. Hong)
- Handling diffusion and stiff source terms with asymptotic preserving properties (joint work with Dr. M. Ding and Dr. R. Shu)
- Nonlinear scalar problems such as the Burgers' equation (joint work with J. Chen, J. Nakao, Dr. Y. Yang)
- Nonlinear hyperbolic systems, such as shallow water, Euler and Navier-Stokes systems.
- Positivity preserving ELDG.
- Moving mesh ELDG method.
- Analysis of stability for nonlinear problems; accurately quantify the time stepping sizes allowed for stability.
- What is the position of semi-Lagrangian schemes in the software development?

References

- An Eulerian-Lagrangian discontinuous Galerkin method for transport problems and its application to nonlinear dynamics, w/ Cai and Yang, JCP, 2021.
- High Order Semi-Lagrangian Discontinuous Galerkin Method Coupled with Runge-Kutta Exponential Integrators for Nonlinear Transport Problems, w/ Cai and Boscarino, JCP, 2021.
- Comparison of semi-Lagrangian discontinuous Galerkin schemes for linear and nonlinear transport simulations, with Cai and Guo, CAMC, accepted.
- A semi-Lagrangian discontinuous Galerkin (DG) - local DG method for solving convection-diffusion-reaction equations, w/ Ding, Cai, Guo, Journal of Computational Physics, JCP, 2020.
- A high order semi-Lagrangian discontinuous Galerkin method for the two-dimensional incompressible Euler equations and the guiding center Vlasov model without operator splitting, with Cai and Guo, JSC, 2019.
- A high order semi-Lagrangian discontinuous Galerkin method for Vlasov-Poisson simulations without operator splitting, with Cai and Guo, JCP, 2018.
- A high order conservative semi-Lagrangian discontinuous Galerkin method for two-dimensional transport simulations, with Cai and Guo, JSC, 2017.

Thank you! Questions?